Onset Voltage of Corona Discharge in Wire-Duct Electrostatic Precipitators

H. Ziedan[1], A. Sayed[1], A. Mizuno[2], and A. Ahmed[1]
[1]Electrical Engineering Department, Assiut University, Egypt
[2]Department of Ecological Engineering, Toyohashi University of Technology, Japan

Abstract—This paper is aimed at investigating how the onset voltage of corona in an electrostatic precipitator is influenced by the number of discharge wires, the wires' radius and the spacing between wires and the collecting plates. The initiation of the corona discharge on the wire surface is located for each wire. The onset voltage is measured for a laboratory model of a precipitator and calculated based on the criterion of self-recurrence of electron avalanches growing in the vicinity of the discharge wires. This calls for calculating the electric field in the vicinity of the discharge wires using the charge simulation method. The calculated onset voltage values agreed reasonably with those measured experimentally.

Keywords—Onset voltage, corona discharge, electric field, electrostatic precipitators

I. INTRODUCTION

In industrial countries, standards were adopted to impose some control over the emission for dark smoke into the atmosphere and, hence, to reduce atmospheric pollution. Electrostatic precipitation [1] is an efficient method of cleaning industrial gases from suspended.

The basic principles governing the operation of electrostatic precipitators are relatively straightforward and are well described in the literature [1, 2]. Conventional duct-type precipitators are made up of a number of discharge wires hanged vertically between grounded collecting plates. A high negative voltage is applied to the discharge wires and negative ions are formed by corona discharge at the wires. These ions accelerate to the collecting plates and charge the particles in their way. When a charged particle reaches the collecting plate, the charge is neutralized and the particle is collected.

An accurate knowledge of the electrostatic field distribution and the onset voltage of corona from the discharge wires is of fundamental importance in developing good models of the different processes that take place in precipitators [3]. Approximate electric field values at the corona onset were calculated in duct-type precipitators with an infinite number of discharge wires at a regular spacing using equations developed before [4]. The voltage that would produce the onset field at the surface of the discharge wires was considered the corona onset voltage and was expressed by an equation for an infinite number of discharge wires at a regular spacing [4].

A method was described [5] for calculating the onset voltage of corona from the discharge wires in duct-type precipitators. The onset voltage was evaluated for the central and the outer wires of a 7-wire precipitator. No attention was forwarded to locate the initiation of the corona discharge on the wire surface as the corona is not initiated at the same point on the discharge wires.

This paper is aimed at investigating how the onset voltage of corona in an electrostatic precipitator is influenced by the number of discharge wires, the wires' radius and the spacing between wires and the collecting plates. The initiation of the corona discharge on the wire surface is located for each wire. The onset voltage is measured for a laboratory model of a precipitator and calculated based on the criterion of self-recurrence of electron avalanches growing in the vicinity of the discharge wires. This calls for calculating the electric field in the vicinity of the discharge wires using the charge simulation method. The calculated onset voltage values agreed reasonably with those measured experimentally.

II. ELECTRIC FIELD CALCILATION

The well-known, charge-simulation technique [6, 7] is used to calculate the electric field for wire-duct ESP with m wires (m is odd). Fig. 1 shows a one-quadrant of the cross-section of the ESP in the X-Y plane. For simplicity, the precipitator is assumed infinitely long the Z-direction. The surface charge on each wire is simulated by (N_1) line charges located at radius rf, where $r_f = f \times r_c$, where f is a fraction, chosen 0.5 in the present work and rc is the radius of discharge wire. The surface charge on each plate of the ESP is simulated by a number (N_2) line charges located outside the plate at a distance from the plate (a) equal to the distance between two adjacent simulation charges (b) as shown in Fig. 1.

Thus, the total number of unknown simulation charges is ($mN_1 + 2N_2$). There is a symmetry around both x- and y- axes, Fig. 1, reduces the number of unknowns to n (= ($mN_1 + 2N_2$)/4).

To evaluate the unknown simulation charges Q_j, j = 1, 2, 3, … , n, a set of boundary points equal to the simulation charges is chosen on the surface of discharge wires and collecting plates as shown in Fig. 1 to satisfy the boundary conditions:

$\Phi = V$ at discharge wires, $\Phi = 0$ at collecting plates

Corresponding author: Hamdy Ziedan
e-mail address: ziedan092@yahoo.com

Received; December 15, 2009

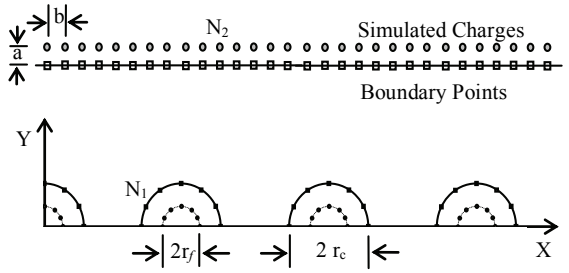

Fig. 1. Arrangement of simulation charges and boundary points for one quarter of a wire duct ESP.

The potential Φ_i is at the ith boundary point of coordinates (x_i, y_i) is the sum of potential contributions due to all simulation charges.

$$\Phi_i = \sum_{j=1}^{n} P_{ij}\, Q_j \tag{1}$$

Where, P_{ij} is the potential coefficient expressed as:

$$P_{ij} = \ln\left(1/R_1 R_2 R_3 R_4\right) \tag{2}$$
$$i = 1, 2, 3, 4, \ldots, n$$
$$j = 1, 2, 3, 4, \ldots, n$$

where,

$$R_1^2 = (x_i - x_j)^2 + (y_i - y_j)^2$$
$$R_2^2 = (x_i + x_j)^2 + (y_i - y_j)^2$$
$$R_3^2 = (x_i + x_j)^2 + (y_i + y_j)^2$$
$$R_4^2 = (x_i - x_j)^2 + (y_i + y_j)^2$$

(x_j, y_j) are the coordinates of the jth simulation charge.

Satisfaction of the boundary conditions at the boundary points formulates a set of equations relating the values of simulation charges to the potential values at the boundary points. This is expressed in a matrix form as:

$$[P]\,[Q] = [V_b] \tag{3}$$

where $[P]$ is the potential coefficient matrix (with dimension $n \times n$), $[Q]$ are unknown simulation charges (with dimension $n \times 1$), and $[V_b]$ are the potential values of the boundary points (with dimension $n \times 1$).

Solution of the set of Eq. (3) determines the unknown simulation charges Q_j.

To check the accuracy of the solution, a set of check points is chosen (each check point is located between two successive boundary points). The potential value is to be checked against the applied value (V at the wire surface and zero at the collecting plates).

Once the accuracy is checked and the simulation charges are known, the electric field intensity at any point p (x_p, y_p) can be determined:

$$E_x = \sum_{j=1}^{n} Q_j \left((x_p - x_j)\left(\frac{1}{R_1^2} + \frac{1}{R_4^2}\right) + (x_p + x_j)\left(\frac{1}{R_2^2} + \frac{1}{R_3^2}\right)\right) \tag{4}$$

$$E_y = \sum_{j=1}^{n} Q_j \left((y_p - y_j)\left(\frac{1}{R_1^2} + \frac{1}{R_4^2}\right) + (y_p + y_j)\left(\frac{1}{R_2^2} + \frac{1}{R_3^2}\right)\right) \tag{5}$$

The magnitude of the electric field intensity at point p is calculated as:

$$E_p = \sqrt{\left(E_x^2 + E_y^2\right)} \quad \text{[V/m]} \tag{6}$$

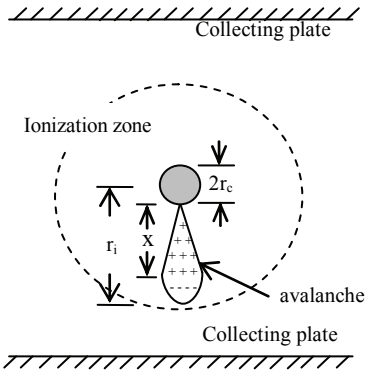

Fig. 2. The development of an avalanche.

III. Corona onset voltage calculation

With the wires of a wire-duct precipitator stressed by negative HV supply, the electric field near a wire reaches the threshold value for ionization of gas molecules by electron collision. A primary electron avalanche starts to develop along the direction of maximum field away from the wire. The avalanche grows through the so-called "ionization zone" whose boundary defines the zone where the ionization coefficient α exceeds the coefficient of electron attachment η, Fig. 2.

In order to simplify the calculations, the following assumptions are made:

1) The ionizing-zone extends from the wire surface to the point where almost all (i.e. 99.99 %) of the electrons get attached to neutral gas molecules and from negative ions.

2) The electron avalanche grows under the influence of its own space-charge field besides the applied electrostatic field.

3) The space-charge-field of the avalanche is the same as if all its positive ions were concentrated at a distance $1/\alpha$ from its tip. This assumption has been found satisfactory in similar work on uniform and nonuniform fields [8].

At the onset voltage, the avalanche should somehow provide an initiating electron at the wire surface to start a successor avalanche, possibly by photoemission, positive ion impact, metastable action or field emission. Field emission is possible only at field strengths exceeding 5×10^7 V/m [9]. Electron emission by positive ion impact is more than two orders of magnitude less probable than photoemission [10]. Metastables have been reported to have an effect approximately equal to that of positive ion impact [11]. Therefore, only the first mechanism (electron emission by photons) was considered in determining the onset voltage.

The condition for a new (successor) avalanche to develop [5, 9] is

$$\gamma_{ph}\left(\int_0^{(r_i - r_c)} \alpha(x)\; e^{\int_0^x (\alpha - \eta)\,dx}\; g(x)\; e^{-\mu x}\; dx\right) \geq 1 \tag{7}$$

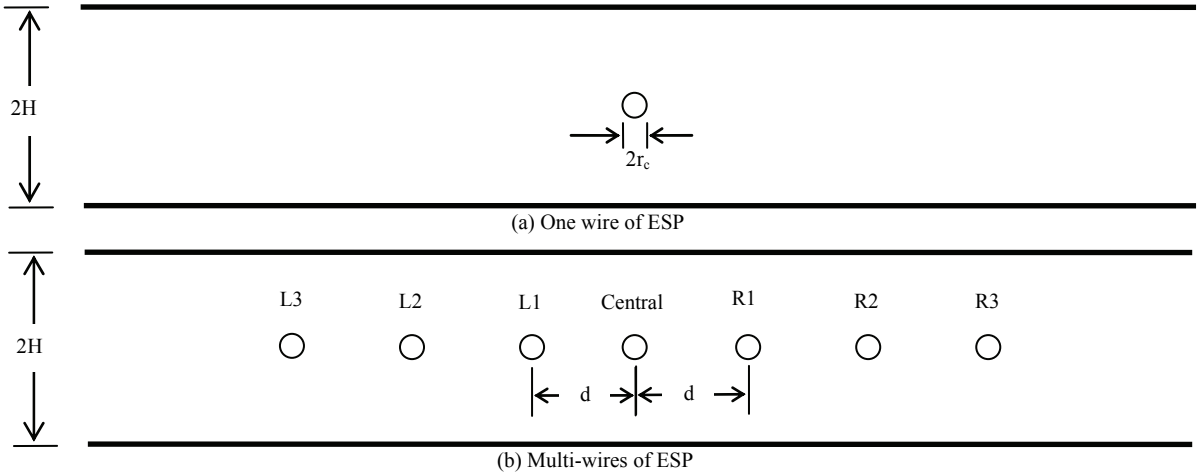

Fig. 3. Configuration of wire-duct ESP.

where

α : Townsend's first ionization coefficient

γ_{ph} : coefficient of electron emission by the action of photons

μ : electron attachment coefficient

$g(x)$:geometry factor to account for the factor that some photons will not be received by the discharge wires of ESP, [5, 9].

The corona onset voltage V_0 does not appear explicitly in last relation, however, the applied voltage affects the values of α, η, ….. The onset voltage V_0 is the critical value which fulfills Eq. (7).

IV. Discharge Parameters

In order to calculate the onset voltage of corona on each wire of the ESP at atmospheric pressure, the relation (7) was solved using the values available in the literature [12], for α, η, γ_{ph} and μ.

The equations relating α [m^{-1}] and η [m^{-1}] at atmospheric pressure to the electric field E [V/m] were expressed as:

$$\eta = 9.8648 - 0.541\times10^{-3}(E) + 11.447\times10^{-3}(E)^2 \quad (8)$$

$$\alpha = 3631.736\, e^{\left(\frac{-167960}{E}\right)} \quad (9)$$

for $19\times10^3 \le (E) \le 45.6\times10^3$

$$\alpha = 7358.32\, e^{\left(\frac{-200792}{E}\right)} + 1.1447\times10^{-8}(E)^2 \quad (10)$$

for $45.6\times10^3 \le (E) \le 182.4\times10^3$

The coefficient of photon absorption μ was taken 500 m^{-1} [12].

The coefficient of electron emission by photons γ_{ph} was taken 3×10^{-3} [12].

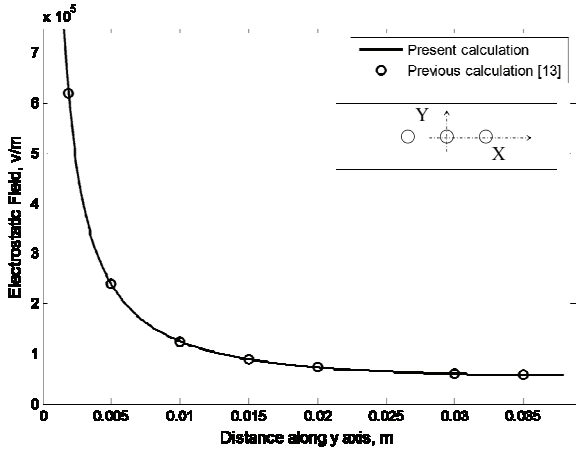

Fig. 4. Electrostatic Field Distribution along y-axis for an applied voltage of 5 kV.

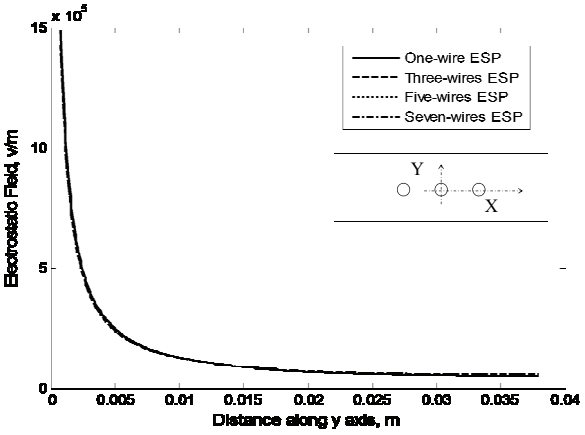

Fig. 5. Electrostatic field distribution along y-axis for ESPs with one-, three-, five- and seven-wires at an applied voltage of 5 kV.

V. Results and Discussion

A. Accuracy of charge simulation technique

The accuracy of charge simulation technique is checked by investigating how the boundary conditions are satisfied in cases of one and multi-discharge wires (3, 5, 7 discharge wires), Fig. 3. It is satisfactory that the maximum percentage error of the calculated surface potential of discharge wires did not exceed 10^{-6} and the maximum percentage error of the calculated surface potential of collecting plates did not exceed 3×10^{-3} (Theoretically, the potential at any point along the

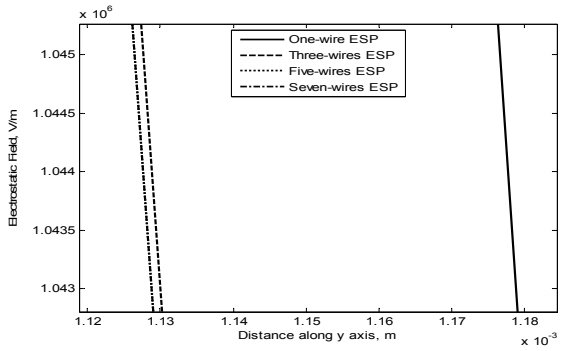

Fig. 6. Electrostatic field distribution along y-axis near the central discharge wire for ESPs with one-, three-, five- and seven-wires at an applied voltage of 5 kV.

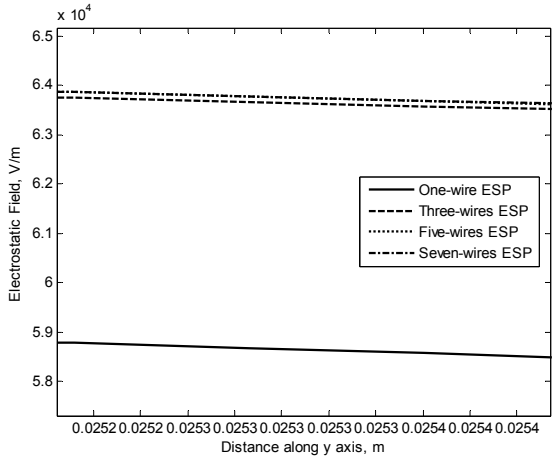

Fig. 7. Electrostatic field distribution along y-axis near the collecting plate for ESPs with one-, three-, five- and seven-wires at an applied voltage of 5 kV.

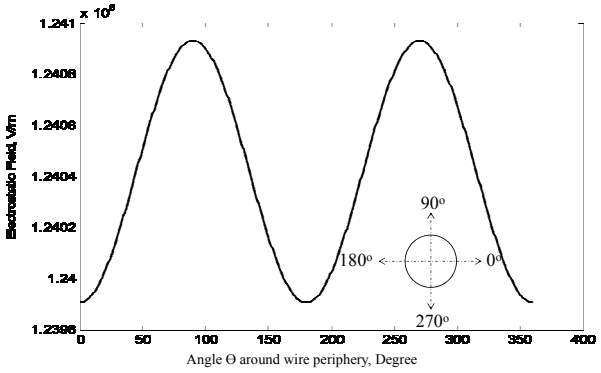

Fig. 8. Electrostatic Field Distribution around the discharge wire for one-wire ESP (at 5 kV).

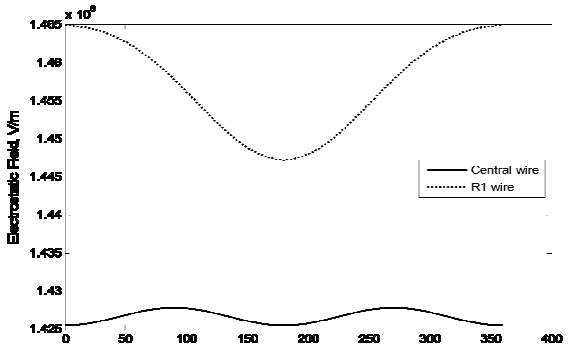

Fig. 9. Electrostatic Field Distribution around the discharge wire for three-wire ESP (at 5 kV).

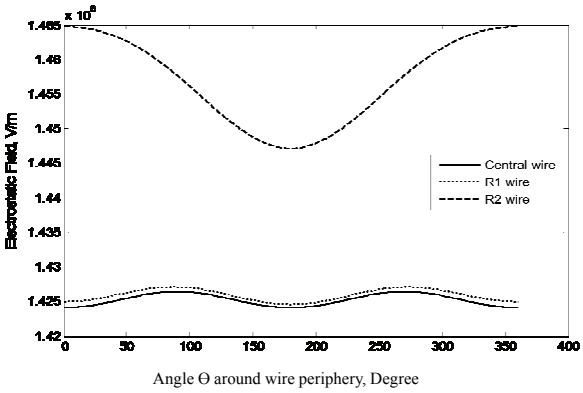

Fig. 10. Electrostatic Field Distribution around the discharge wire for five-wire ESP (at 5 kV).

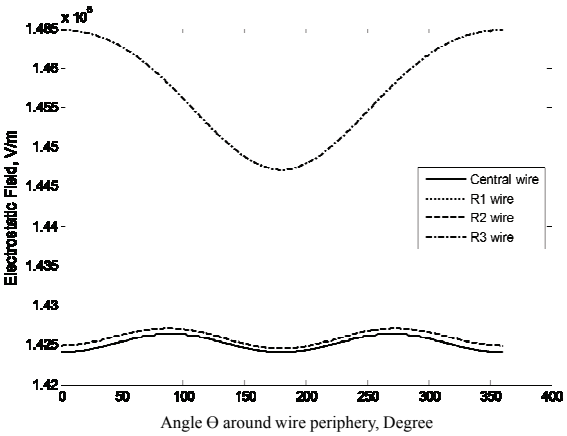

Fig. 11. Electrostatic Field Distribution around the discharge wire for seven-wire ESP (at 5 kV).

collecting plates should be zero) irrespective of the number of discharge wires and ESP geometry (wire radius r_c, wire-to-wire spacing d and wire-to-plate spacing H of ESP).

The discharge wires of ESP (in case of multi-discharge wires) are arranged in a row equidistant from the two collecting ground plates. All the wires have the same applied voltage and the same diameter. For comparison purpose, the wire-duct ESP parameters as reported in the literature [13], (r_c = 0.825 mm, d = 7.6 cm, and H = 3.8 cm) are considered. The decrease of the electrostatic field intensity along the vertical axis of symmetry (y-axis) is shown in Fig. 4 for applied voltage of 5 kV (less than the onset voltage). It is quit clear that all the present calculations agreed well with those reported before [13]. This confirms the accuracy of the present calculations.

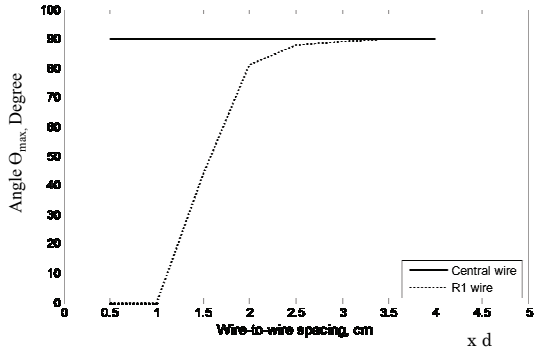

Fig. 12. Variation of angle Θ_{max} with the wire-to-wire spacing of three-wires ESP.

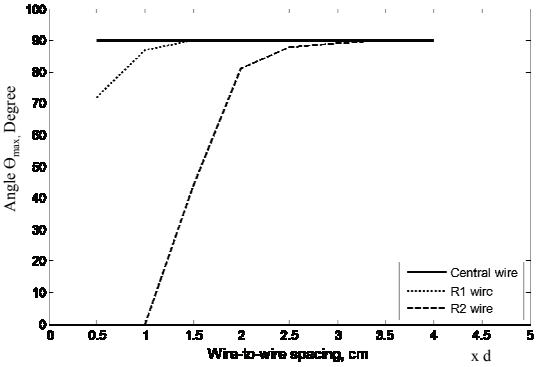

Fig. 13. Variation of angle Θ_{max} with the wire-to-wire spacing of five-wires ESP.

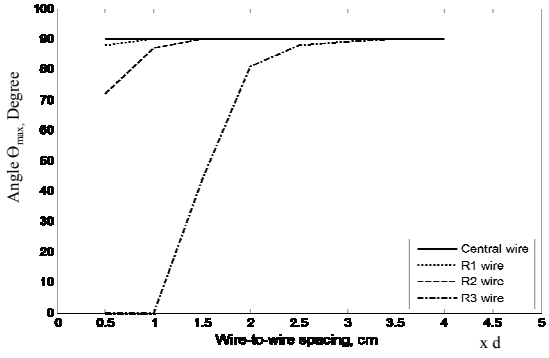

Fig. 14. Variation of angle Θ_{max} with the wire-to-wire spacing of seven-wires ESP.

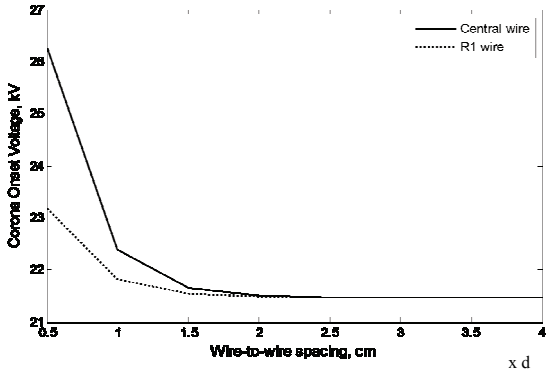

Fig. 15. Variation of corona onset voltage with the wire-to-wire spacing of three-wires ESP.

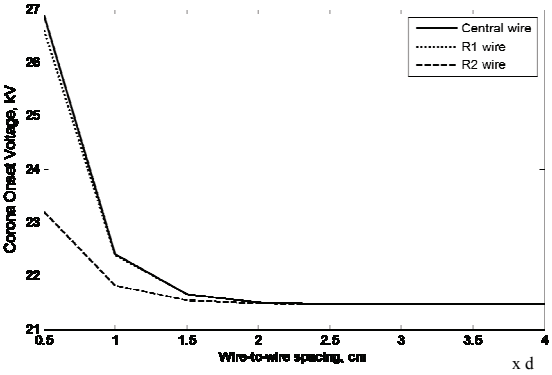

Fig. 16. Variation of corona onset voltage with the wire-to-wire spacing of five-wires ESP.

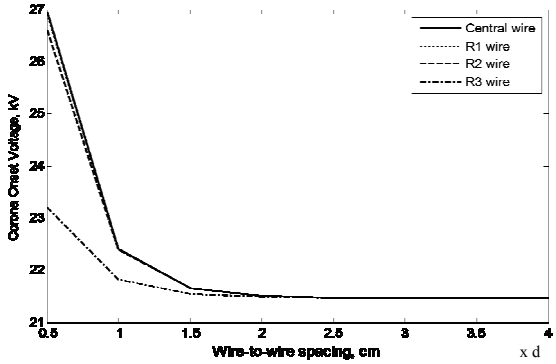

Fig. 17. Variation of corona onset voltage with the wire-to-wire spacing of seven-wires ESP.

B. Electrostatic Field along ESP axis

The electrostatic field intensity along the ESP axis (Y-axis) starting from the surface of the central discharge wire up to collecting plate is shown in Fig. 5 for ESPs with one-, three-, five- and seven-discharge wires. It is clear that the field near the central discharge wire in case of one-discharge wire ESP is higher than that for ESP with multi-wires. This is simply explained by the shielding effect imposed on the central wire due to other wires, Figs. 5 and 6. On the other hand, the field near the collecting plate for one wire ESP is smaller than that for ESP with multi-wires, Figs. 5 and 7. This conforms to the fact that the voltage applied to the discharge wires is the same, so the line integral of the field value from the central wire surface up to the collecting plate should be the same whatever the number of discharge wires.

C. Electrostatic Field around Discharge Wires

Electrostatic field distributions around the discharge-wires of different ESP configurations are shown in Figs. 8-11. In all ESP configurations, the electrostatic field around the outer wire is higher than that around the other (inner) wires. This is because the inside wires are shielded by the outer wires.

TABLE I
CALCULATED CORONA ONSET VOLTAGE VALUES FOR DIFFERENT ESP CONFIGURATION

	Corona onset Voltage, kV			
	Central-wire	R1-wire	R2-wire	R3-wire
1-wire ESP	21.464	--------	--------	--------
3-wires ESP	22.383	21.817	--------	--------
5-wires ESP	22.404	22.394	21.817	--------
7-wires ESP	22.405	22.404	22.394	21.817

TABLE II
VARIATION OF ANGLE Θ_{max} AND ONSET VOLTAGE OF CORONA ON THE DISCHARGE WIRES AS INFLUENCED BY THE WIRE-TO-WIRE SPACING OF THREE-WIRE ESP

wire-to-wire spacing, cm	Central wire		Right (outside) wire	
	Θ_{max}	$V_{onset, kV}$	Θ_{max}	$V_{onset, kV}$
0.5×d	90	26.273	0	23.178
1.0×d	90	22.383	0	21.817
1.5×d	90	21.652	44	21.551
2.0×d	90	21.503	81	21.483
2.5×d	90	21.473	88	21.468
3.0×d	90	21.466	89	21.465
3.5×d	90	21.465	90	21.465
4.0×d	90	21.465	90	21.465

TABLE III
VARIATION OF ANGLE Θ_{max} AND ONSET VOLTAGE OF CORONA ON THE DISCHARGE WIRES AS INFLUENCED BY THE WIRE-TO-WIRE SPACING OF FIVE-WIRE ESP

wire-to-wire spacing, cm	Central-wire		R1-wire		R2-wire	
	Θ_{max}	$V_{onset, kV}$	Θ_{max}	$V_{onset, kV}$	Θ_{max}	$V_{onset, kV}$
0.5×d	90	26.888	72	26.599	0	23.199
1.0×d	90	22.404	87	22.394	0	21.817
1.5×d	90	21.653	90	21.653	44	21.551
2.0×d	90	21.504	90	21.504	81	21.484
2.5×d	90	21.473	90	21.473	88	21.469
3.0×d	90	21.467	90	21.467	89	21.466
3.5×d	90	21.466	90	21.466	90	21.465
4.0×d	90	21.466	90	21.466	90	21.466

TABLE IV
VARIATION OF ANGLE Θ_{max} AND ONSET VOLTAGE OF CORONA ON THE DISCHARGE WIRES AS INFLUENCED BY THE WIRE-TO-WIRE SPACING OF SEVEN-WIRE ESP

wire-to-wire spacing, cm	Central wire		R1-wire		R2-wire		R3-wire	
	Θ_{max}	$V_{onset, kV}$	Θ_{max}	$V_{onset, kV}$	Θ_{max}	$V_{onset, kV}$	Θ_{max}	$V_{onset, kV}$
0.5×d	90	26.956	88	26.925	72	26.602	0	23.199
1.0×d	90	22.405	90	22.404	87	22.394	0	21.817
1.5×d	90	21.653	90	21.653	90	21.653	44	21.551
2.0×d	90	21.503	90	21.503	90	21.503	81	21.484
2.5×d	90	21.473	90	21.473	90	21.473	88	21.469
3.0×d	90	21.467	90	21.467	90	21.467	89	21.466
3.5×d	90	21.465	90	21.465	90	21.465	90	21.465
4.0×d	90	21.465	90	21.465	90	21.465	90	21.465

TABLE V
CALCULATED AND MEASURED CORONA ONSET VOLTAGE FOR ONE-WIRE ESP

Wire radius, mm	$V_{onset-calc,}$ kV	$V_{onset-measured,}$ kV			
		Grounding circuit		HV circuit	
		Average Value	Standard Div., kV	Average Value	Standard Div., kV
0.250	16.070	15.984	± 0.128	15.952	± 0.148
0.365	19.930	19.792	± 0.150	19.792	± 0.180
0.500	23.931	23.698	± 0.290	23.860	± 0.450

D. Corona Onset Voltage Calculation

The proposed criterion (7) is applied for different ESP configurations with 1, 3, 5 and 7 discharge wires. The calculated onset voltage values of corona on each wire are given in Table I.

It is quite clear that the onset voltage is higher for the central wire and decreases for wires in the direction toward the end of the collecting plates. This is because the central wire is fully shielded by the other wires at stated above with a subsequent decrease of the field at its surface. At the central wire, the onset voltage increases

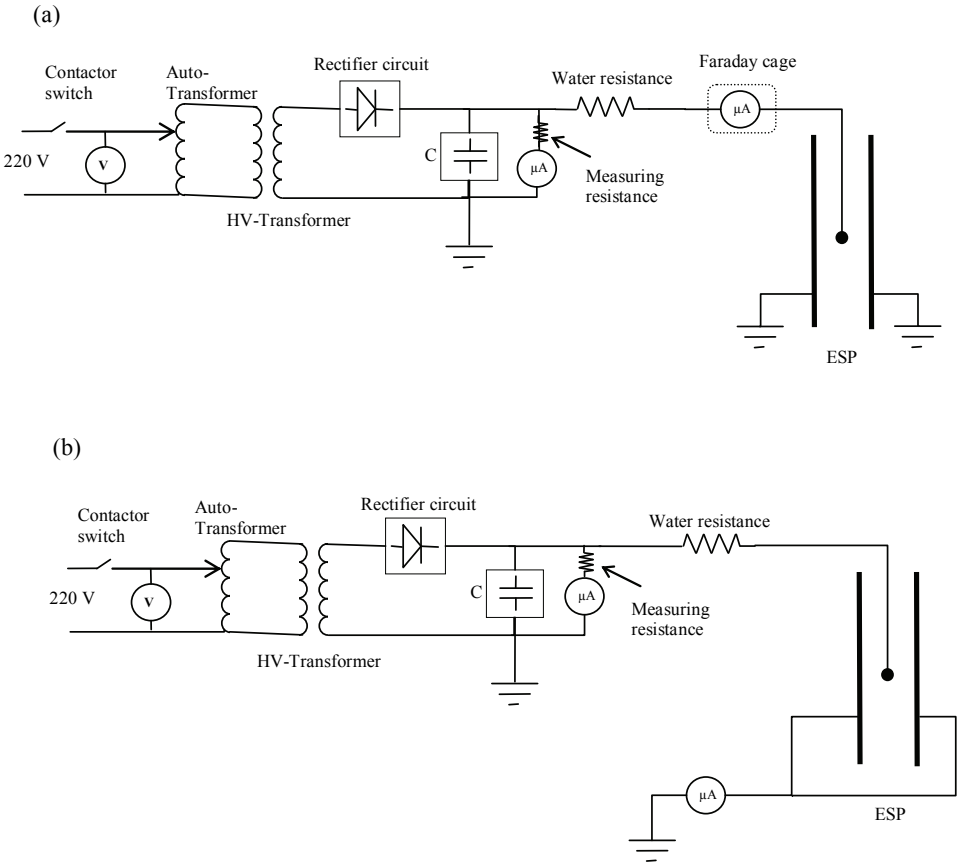

Fig. 18. Variation of corona onset voltage with the wire-to-wire spacing of seven-wires ESP.
(a) In the high circuit. (b) In the ground circuit.

TABLE VI
CALCULATED AND MEASURED CORONA ONSET VOLTAGE FOR THREE-WIRE ESP.

	r = 0.25 mm			r = 0.5 mm		
	$V_{onset-calc,}$ kV	$V_{onset-measured,}$ kV		$V_{onset-calc,}$ kV	$V_{onset-measured,}$ kV	
		Average Value	Standard Div., kV		Average Value	Standard Div., kV
Central-wire	24.008	24.146	± 0.27	37.224	37.000	± 0.31
Right-wire	21.062	20.812	± 0.33	31.805	31.528	± 0.38
Left-wire	21.062	20.900	± 0.31	31.805	31.639	± 0.36

TABLE VII
CALCULATED AND MEASURED CORONA ONSET VOLTAGE FOR FIVE-WIRE ESP.

	r = 0.25 mm			r = 0.5 mm		
	$V_{onset-calc,}$ kV	$V_{onset-measured,}$ kV		$V_{onset-calc,}$ kV	$V_{onset-measured,}$ kV	
		Average Value	Standard Div., kV		Average Value	Standard Div., kV
Central-wire	28.829	28.660	± 0.29	45.237	45.036	± 0.33
R1-wire	27.356	27.352	± 0.31	42.601	42.056	± 0.42
L1-wire	27.356	27.250	± 0.29	42.601	42.120	± 0.43
R2-wire	22.430	22.400	± 0.39	33.858	33.796	± 0.54
L2-wire	22.430	22.380	± 0.40	33.858	33.590	± 0.52

with the increase of the number of discharge wires, Table I as the shielding effect becomes more pronounced with the increase of the number of discharge wires, Table I.

The angle of maximum electrostatic field (Θ_{max}) around the periphery of discharge wires depends on the ESP configuration. This angle defines where the primary avalanche grows in the vicinity of the discharge wires. It is mainly influenced by the wire-to-wire spacing. The angle Θ_{max} is equal 90^o for the central wire, 0^o for the outer wire and has a value between 90^o and 0^o for other wires. With the increase of the wire-to-wire spacing, Θ_{max} of all wires tends to approach 90^o. This corresponds to the case where each wire behaves separately with no interaction among the wires as given in Tables II-IV and shown in Figs. 12-14.

The onset voltage values of corona on the discharge wires of ESP depend on the wire-to-wire spacing for the same wire radius and wire-to-plate spacing. The onset voltage is higher for corona on the central wire when compared with other wires, Figs. 15-17. This is attributed to the decrease of the field in the vicinity of the central wire due to the above mentioned shielding effect by the other wires. With the increase of the wire-to-wire spacing, the onset voltage decreases because of the less shielding effect and associated decreasing of the field in the vicinity of discharge wires. With further increase of the wire-to-wire spacing, the onset voltage approaches the same value for all discharge wires where each wire behaves separately with no interaction (shielding) among wires, Figs. 15-17.

The difference between the corona onset voltage of the outer wire and that of the central wire decreases with the increase of the wire-to-wire spacing, Tables I-IV and Figs. 15-17. However, the difference is so small that the effect of the space charge from the coronating wire on changing the surface field of the non-coronating wires is negligible with respect to the electrostatic field due to the applied voltage. This is the only simplifying assumption adopted in the present study.

VI. Experimental validation results

A. Experimental Setup

A wire-duct electrostatic precipitator (ESP) was set-up in the HV laboratory of Assiut University to compare the calculated and measured corona onset voltage values for different ESP configurations.

The set-up consists of:

1) A regulating transformer with 220-V ac input voltage feeds a variable supply voltage to the high-voltage transformer through a contactor switch.

2) HV transformer steps the voltage up to the desired value in the range 0 - 100 kV for rectification. A half-wave HV rectifier circuit composed of two 20-mA, 140 kV PIV diodes and 1 nF, 140 kV smoothing capacitor generates a variable dc voltage in the range 0-140 kV. The dc voltage is applied across a 280-MΩ resistance in series with a micro-ammeter for measuring the generated dc voltage. This voltage is applied to the investigated duct-wire ESP through a 0.5 MΩ water-resistance. The water-resistance is to limit the current in case of a flash happens in ESP.

3) The discharge wires of the ESP are copper conductors with diameters of 0.5, 0.73 and 1.0 mm. The wires are hinged vertically between two collecting plates. Each wire is terminated at both ends by two smoothing copper spheres to avoid field concentration. The top ends of the wires are stressed through a smooth copper strip connection. Wire-to-wire spacing is maintained constant at 6.3 cm.

4) The collecting plates forming the duct of the ESP are made of steel and hanged vertically by a wooden support. The dimensions of each plate are 1-m height and 1-m length. Plate-to-plate distance is maintained constant at 28.9 cm.

5) A Faraday's cage is used to shield a digital micro-meter for recording corona currents in discharge wires.

B. Experimental Technique

To measure the onset voltage from each discharge wire, the shielded micro-ammeter is connected to the discharge wire and the corona current is recorded with the increase of the applied voltage. The onset voltage corresponds to the applied voltage when the micro-ammeter starts to record a reading just above the zero value.

C. Calculated Onset voltages against Those Measured Experimentally

Table V gives the calculated and measured values of the corona onset voltage in an ESP with one discharge wire as influenced by the wire radius. The measured values were recorded when the digital micro-ammeter was connected in the ground and high-voltage circuits, Fig. 18. It is quite clear that the calculated values agreed reasonably with those measured experimentally. The measured values are almost the same irrespective of the connection of the micro-ammeter in the ground and high-voltage circuits. The higher the wire radius the higher is the corona onset voltage. This is simply attributed to the decrease of the electric field at the wire surface and its vicinity with the increase of the wire radius.

Tables VI and VII give the calculated and measured values of the corona onset voltage in ESP's with 3 and 5 discharge wires for two different values of the wire radius. Again, the calculated values agreed reasonably with those measured experimentally. The dependency of the onset voltage on the wire radius is the same as discussed for the ESP with one discharge wire. The onset voltage is higher for corona on the central discharge wire when compared with other wires, Tables VI and VII. This is attributed to the decrease of the field in the vicinity of the central wire because of the shielding effect imposed by the other wires as stated above in section V-D. The onset voltage decreases gradually starting from central wire reaching its minimum value for the outer discharge wires. This is because the above-mentioned shielding effect decreases gradually in the direction away from the central wires with a subsequent increase of the electric field and decrease of the onset voltage as depicted in Tables VI and VII.

VII. Conclusion

(1) The field near the central discharge wire in case of one-discharge wire ESP is higher than that for ESP with multi-wires due to the shielding effect imposed on the central wire due to the other wires.

(2) The calculated electric field along the ESP axis

decreases away from the discharge wire in agreement with previous calculation.

(3) In all ESP configurations, the electrostatic field around the outer wire is higher than that around the other (inner) wires. This is because the inside wires are shielded by the outer wires.

(4) The angle of maximum electrostatic field (Θ_{max}), which defines where the primary avalanche grows, is influenced by the wire-to-wire spacing. The angle Θ_{max} is equal 90^o for the central wire, 0^o for the outer wire and has a value between 90^o and 0^o for other wires.

(5) With the increase of the wire-to-wire spacing, Θ_{max} of all wires tends to approach 90^o. This corresponds to the case where each wire behaves separately with no interaction among the wires.

(6) The onset voltage of corona in electrostatic precipitators with 1, 3 and 5 discharge wires is calculated and measured in the laboratory. The calculated values agreed reasonably with those measured experimentally.

(7) The onset voltage increases with the increase of the radius of discharge wires for the same wire-to-wire and collecting plate-to-plate spacings.

(8) The onset voltage increases gradually in the direction away from the central discharge wire reaching its maximum value at the central wire and minimum value at the outer wires.

ACKNOWLEDGMENT

The authors would like to thank Prof. Mazen Abdel-Salam of Assiut University, Egypt for his interest in this research work.

REFERENCES

[1] J. M. Robinson, "Electrostatic precipitation," in *Electrostatics and its Applications*. A. D. Moore, New York, NY: Wiley, 1978, pp. 180-220.

[2] S. Oglesby and G. B. Nichols, *Electrostatic Precipitation*. New York, NY: Marcel Dekker, 1978, pp. 10-11.

[3] K. J. McLean, "Electrostatic precipitators," *IEE Proceedings A, Science, Measurement and Technology*, vol. 135, pp. 347-361, 1988.

[4] S. Sekar and H. Stomberg, "On the prediction of current-voltage characteristics for wire plate precipitators," *Journal of Electrostatics*, vol. 10, pp. 35-43, 1981.

[5] M. Abdel-Salam and D. Wiitanen, "Calculation of corona onset voltage for duct-type precipitators," *IEEE Transactions on Industry Applications*, vol. 29, pp. 274-280, 1993.

[6] M. Abdel-Salam, "Electric Fields," in *High Voltage Engineering Theory and Practice*. M. Abdel-Salam, H. Anis, A. E. Morshedy, R. Radwan, New York, NY: Marcel Dekker, 2000, pp. 9-80.

[7] H. Singer, H. Steinbigler, and P. Weiss, "A Charge Simulation Method for the Calculation of High Voltage Fields," *IEEE Transactions on Power Apparatus and Systems*, vol. PAS-93, pp. 1660-1668, 1974.

[8] K. Honda, "On a Streamer Breakdown Criterion of a Uniform Air Gap" (in Japanese), *The Journal of the Institute of Electrical Engineers of Japan*, vol. 85, pp. 1394-1401, 1965.

[9] M. Abdel-Salam and K. Stanek, "On the calculation of breakdown voltages for uniform electric fields in compressed air and SF6," *IEEE Transactions of Industry Applications*, vol. 24, pp. 1025-1030, 1988.

[10] L. B. Loeb, *Electrical Coronas: Their Basic Physical Mechanisms*. Berkely, CA: University of California Press, 1965, pp. 299-359.

[11] M. Abdel-Salam, *Ionization and deionization processes in gases*, in *High Voltage Engineering Theory and Practice*. M. Abdel-Salam, H. Anis, A. E. Morshedy, R. Radwan, New York, NY: Marcel Dekker, 2000, pp. 81-112.

[12] M. P. Sarma and W. Janischewskyj, "D.C. corona on smooth conductors in air. Steady-state analysis of the ionisation layer," *Proceedings of the Institution of Electrical Engineers*, vol. 116, pp. 161-166, 1969.

[13] A. A. Elmoursi and G. S. P. Castle, "Modeling of corona characteristics in a wire-duct precipitator using the charge simulation method," *IEEE Transactions on Industry Applications*, vol. 23, pp. 95-102, 1987.